OPEN ACCESS

University of BRISTOL

Humphreys, D., Raffo, A., Bosi, G., Vannini, G., Schreurs, D., Gebremicael, K. N., & Morris, K. (2016). Maximizing the benefit of existing equipment for nonlinear and communication measurements. In *Proceedings of the 2016 87th ARFTG Microwave Measurement Conference (ARFTG)* https://doi.org/10.1109/ARFTG.2016.7501962

Peer reviewed version

Link to published version (if available):
10.1109/ARFTG.2016.7501962

Link to publication record in Explore Bristol Research
PDF-document

This is the author accepted manuscript (AAM). The final published version (version of record) is available online via IEEE at http://ieeexplore.ieee.org/document/7501962/. Please refer to any applicable terms of use of the publisher.

University of Bristol - Explore Bristol Research
General rights

This document is made available in accordance with publisher policies. Please cite only the published version using the reference above. Full terms of use are available:
http://www.bristol.ac.uk/red/research-policy/pure/user-guides/ebr-terms/

Maximizing the Benefit of Existing Equipment for Nonlinear and Communication Measurements

David A. Humphreys[1,4], Antonio Raffo[2], Gianni Bosi[2,3], Giorgio Vannini[2], Dominique Schreurs[3], Kibrom N. Gebremicael[4] and Kevin Morris[4]

[1]National Physical Laboratory, Teddington, UK, [2]Engineering Department, University of Ferrara, 44122 Ferrara, Italy, [3]Div. ESAT-TELEMIC, KU Leuven, B-3001 Leuven, Belgium, [4]Communications Systems and Network Group, University of Bristol, Bristol, UK.

***Abstract* — The Nonlinear Vector Network Analyzer (NVNA) is the workhorse for nonlinear measurements. Also, during the development of new communications systems, such as 5G, dedicated test equipment is not available. Sampling and real-time oscilloscopes offer a lower cost alternative to the NVNA but require error corrections to improve their accuracy. NPL, NIST and other NMIs have advanced this area and we summarize these corrections and their limitations, with examples, and set out guidance rules to maximize the accuracy of the results.**

***Index Terms* — Nonlinear measurements, oscilloscope, sampling, analog to digital conversion**

I. Introduction

Improving efficiency and linearity though nonlinear design and waveform engineering techniques is essential for current and future communication systems and the Nonlinear Vector Network Analyzer (NVNA), coupled with impedance synthesis are key instruments for component and subsystem characterization. However, these systems are costly and may not be available for budgetary reasons. Similarly, during the development of a new communications environment, such as 5G, the dedicated test equipment cannot be developed and made available until the standards have been agreed.

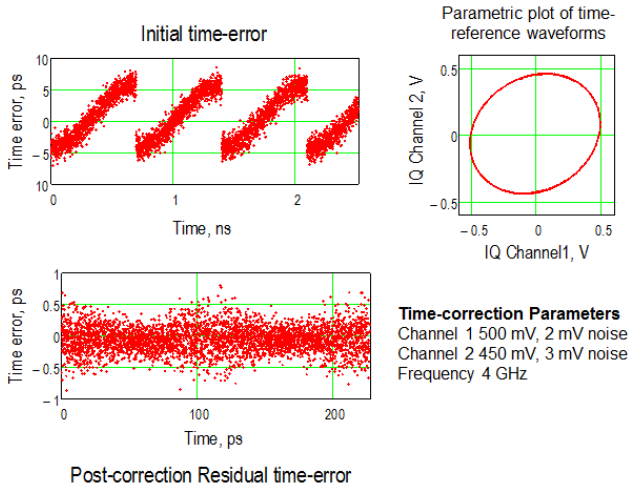

Fig 1. In-phase and quadrature (IQ) timebase correction using simulated data with unequal channel noise. The timing errors are reduced to the sub-picosecond level but the residual timing errors show periodic modulation at the IQ frequency.

In order to verify simulation results by measurement a stop-gap solution based on general equipment is required. Real-time oscilloscope (DRTO) and equivalent-time (sampling) oscilloscopes (DSO) can be used as an alternative for some applications but these instruments contain impairments that must be corrected to achieve the best results. The corrections process is imperfect and will introduce secondary errors into the result. Understanding the nature of the secondary errors allows intelligent choices for the correction frequencies to minimize the impact of the errors on the result. There is also a balance to be struck between the measurement duration and the volume of data in the results and the accuracy improvement. Solutions that are too slow or create too much data will be quickly abandoned.

In this paper we consider the instruments architecture, timebase errors, amplitude errors, the correction algorithms, and the secondary errors associated with frequency choices. These results are backed up by measurement examples.

II. Instrument Architectures and Impairments

The DSO is a much older architecture but at present it provides the link to disseminate traceable dynamic electrical quantities from the physics-based primary standards that have been realized through Electro-optic sampling (EOS) [1] - [3]. The DRTO is a more recent development and has rapidly advanced so that the state-of-the-art instruments now have a comparable bandwidth to the best DSOs.

Timing errors affect the frequency-domain results because the orthogonality condition, fundamental to the Fourier transform, is broken. This increases the noise-floor.

A. Digital Sampling Oscilloscope

Each channel of a DSO contains a single sampling gate per channel and a single sample is taken on each channel for every valid trigger event. For many instruments all the channels are triggered simultaneously and this is used as the basis for the timebase correction. An individual sweep may contain over ten-thousand samples and so if the frame rate is low this will affect the acquisition time. For example, a single sweep of a communications system waveform with a 10 ms frame rate would take over 100 seconds. This provides a practical limitations to its use in many applications.

The timebase of these instruments is poor when compared with the microwave equipment but because of their role in primary standard dissemination and a using feature of the sampling-gate architecture, timebase correction algorithms have been developed [4] - [6] but their effectiveness is design dependent [7]. Hardware solutions are also available but in both cases two instrument channels must be sacrificed to provide this functionality.

Two RF signals, nominally at quadrature, phase-locked to the waveform under test and harmonically related to the trigger signal provide the timing reference. However, these waveforms will have some impairments, such as noise, imperfect phase alignment and residual harmonic component. The noise components may differ between the two reference channels and give rise to periodic modulation of the time uncertainty (Fig. 1). This problem can be overcome by ensuring that the two sampler channels are well matched, the reference signals are equal, harmonic-free and at quadrature.

Uncorrected harmonic errors can provide a periodic modulation of the timebase and a consequential phase modulation of the measurement waveform, creating modulation sidebands,

$$f_{IM}(h_1, h_2) = h_1 f_0 \pm h_2 f_{IQ}, \quad (1)$$

where $h_1$and h_2 are the harmonic indices for the components of f_0 and f_{IQ} respectively.

For applications such as nonlinear device measurement where the magnitude and phase of the harmonics is critical, using a reference signal that is harmonically related to the fundamental will introduce ambiguity in the results as the modulation terms will add to adjacent harmonics. This problem can be avoided by using a sub-harmonic trigger

$$f_{trig} = \frac{f_0}{n_{div}}, \quad (2)$$

where f_0 is the fundamental frequency and n_{div} is the division ratio. The reference frequency will be harmonically related to the trigger as

$$f_{IQ} = m.f_{trig}, \quad (3)$$

where f_{IQ} and ½f_0 are not harmonically related.

B. Digital Real-Time Oscilloscope

The DRTO acquires the full waveform in a single sweep so the trigger-rate does not present an issue. However, these instruments can generate very large data-files. For example, to fully represent a 2 GHz carrier, communications waveform with 20 MHz bandwidth would require a sampling rate of at least 4 GSa/s and so a 1 ms epoch acquired at 5 GSa/s would yield a data set of 5 M data points. The size of this data-set can be reduced by undersampling or by post-processing as both communications waveforms and nonlinear device measurements are sparse when viewed in the frequency domain.

To achieve the required data acquisition rate the system comprises many individual ADCs, typically with 8-bit resolution. There are also some lower bandwidth 12-bit instruments available. The individual ADCs will have a slight variation in their dc levels, scale-factor and frequency response, giving rise to sub-Nyquist spur components [8].The lowest sub-harmonic (f_{sp}) will be at a frequency

$$f_{sp} = \frac{S}{m}, \quad (4)$$

where S is the sampling frequency and m is the number of ADCs. There will be interference components at all the harmonics of f_{sp} up to the Nyquist frequency.

There have been several papers describing calibration algorithms for these instruments and identifying systematic errors such as inter-channel delay and range-dependent timing changes [9] – [11]. Although these algorithms are targeted at instrument calibration can be readily adapted to maximize the accuracy of a device or sub-system measurement.

The DRTO can normally be phase-locked to the synthesizers used to generate the stimulus waveform. The quality of the phase-locking determines epoch useable without correction to avoid truncation errors that will introduce spurious frequency components. This can be determined from a long-epoch measurement of a CW RF waveform and Allan deviation analysis of the result [9].

In addition to ADC spurs it is important to avoid ADC prime-number sub-Nyquist frequencies as these will always correspond to the same ADC levels but not necessarily the same ADCs. If the stimulus frequency is slightly offset from the sub-Nyquist components then over a period t_{block}, where

$$t_{block} = \frac{1}{|f_{stim} - f_{subNQ}|}, \quad (5)$$

and the frequencies correspond to the stimulus (f_{stim}) and the sub-Nyquist (f_{subNQ}) tones, the samples will exercise different ADC levels reducing the measurement uncertainties and the waveform becomes heavily oversampled providing temporal detail. For measurements at multiple frequencies the values can me computed in advance and stored in a look-up table.

The prime-number algorithm used in the example selects frequencies that are as close to the desired frequency whilst avoiding the sub-Nyquist components [9]. The number of samples in the block (P) and the number ADCs (n_{ADC}) must contain no common prime factors. Also the number of samples in the block (P) and the number of waveform periods (R) for the fundamental and all the harmonics under consideration must contain no common prime factors. There are a number of block-length and prime-number combinations that will give a result that is close to the target frequency and the figure of merit (F_{pr}) to rank the suitable combinations of P and R, is

$$F_{pr} = \frac{1}{\sum_i p_i + \sum_k r_k}, \quad (6)$$

where each prime factor p of P and r of R is counted only once. This will bias the selection against large prime values.

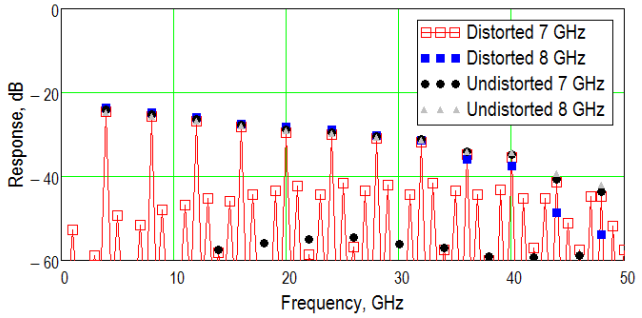

Fig. 2 IQ reference distortion creates IM products on the measured comb waveform. Choice of IQ frequency is important to avoid systematic errors.

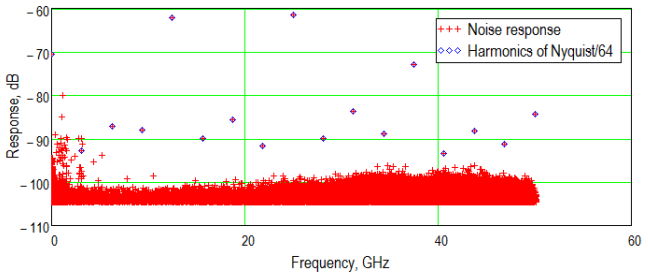

Fig. 3. Noise response of 50 GHz, 200 GSa/s DRTO showing the sub-Nyquist noise spurs corresponding to 64 ADCs

III. DSO Measurement Example

We measured an RF phase standard at 4 GHz repetition rate as a test example. The 500 MHz trigger signal was derived from the same source and using a fast divider circuit. This allows the In-phase and quadrature and reference signals (IQ) to be locked to a sub-harmonic of waveform under test (see (1) - (3)).

The sampling head used for the IQ signals was deliberately chosen as its poor vertical-scale linearity which can be varied by altering the dc bias-point. A 90-degree hybrid coupler was used to generate near quadrature components. The residual periodic modulation of the timebase due to the harmonics of the IQ waveforms will result in intermodulation products in the result (1). If these two frequencies are harmonically related then the IM components will cause a systematic error in the measurement result. This is illustrated in Fig. 2 for IQ frequencies of 7 GHz and 8 GHz. The resulting IM products from the 7 GHz IQ measurement fall in between the comb lines and can therefore be corrected whereas the components at from the 8 GHz IQ measurement cause a systematic distortion term. Even with a mathematical correction, there will remain a residual periodic uncertainty term in the result and so this is best avoided by ensuring the purity of the reference signal and the linearity of the sampler.

IV. DRTO Measurement Example

Measurements of a nonlinear amplifier at a nominal target frequency of 10 GHz have been performed using a 50 GHz DRTO operating at 200 GSa/s. Measurements of a single acquisition noise trace (no applied signal or averaging) show that the instrument has 64 ADCs (Fig. 3). The clock stability was verified at 2.06 GHz and the Allan deviation shows that the timebase remains accurately locked at epochs of at least one microsecond.

The choice of frequency for the prime-number algorithm are shown in Table I.

TABLE I
FREQUENCY SELECTION FOR DIFFERENT MEASUREMENT STRATEGIES

	Prime number	Exact
Number of samples per block	8281	20
Prime factors	7, 13	2, 5
Number of waveform repeats	2070	1
	2, 3, 5, 23	1
Frequency (GHz)	9.998 792	10.0
Frequency error (MHz)	-1.2	-
Effective sampling rate (TSa/s)	82.8	0.2

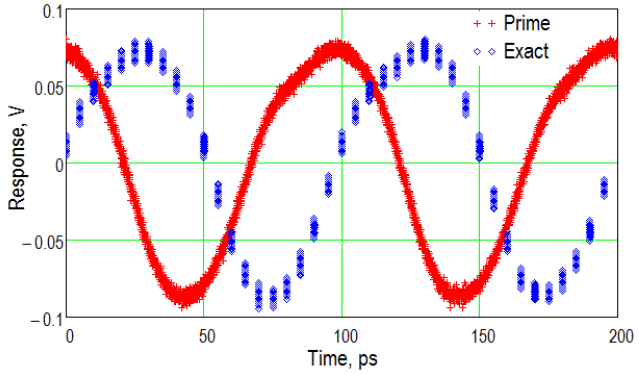

Fig. 4. Distorted waveform from an amplifier measured using the exact target frequency the prime-number sampling strategy.

The DRTO used for this work has a higher oversampling ratio than other commercially available instruments. Despite this, the measurement trace data in the time-domain shows that under normal operation, the “exact” sampling case, the highest harmonic under consideration (50 GHz) will only be represented by four points. However, the prime-number algorithm measures at a frequency that is offset by 15 MHz below the 10 GHz target and the resulting oversampling is sufficient to exercise all available ADC levels (fig.4).

In the frequency domain, the two strategies show good agreement but at 50 GHz the 5th harmonic of the waveform is coincident with a sub-Nyquist tone (fig. 5).

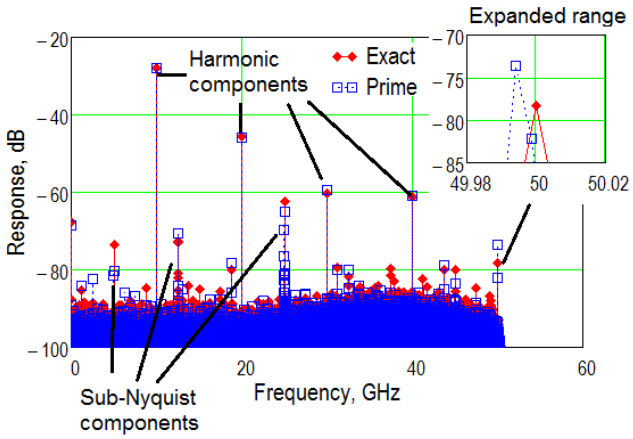

Fig. 5 Frequency components of the distorted signal show good agreement for the two sampling strategies except at 50 GHz.

V. Communications Waveform Example

Communication waveforms are sparse in terms of the instrument bandwidth but are locally very dense about the carrier frequency. Undersampling is important for reducing the computational workload and improving energy efficiency.

In the measured waveform, the desired LTE signals are at 850 MHz and 2 GHz (Fig. 6). The waveform was acquired using a DRTO with 10 GSa/s and the sub-Nyquist sampling of the resulting waveform was performed using the algorithm outlined in [12] using *Modulated Wideband Converter* (MWC) sampling in which the individual ADCs are sub-harmonically related to the Nyquist frequency. This can be achieved by taking the n^{th} and m^{th} samples (n and m are not equal) of a waveform acquired by the RTDO.

As we have seen earlier, the RTDO contains many ADCs and therefore at each rate associated with the MWC sampling a different pattern of ADCs will be used. The most benign case will be when only one ADC is in play (4). At all other frequencies an additional error will be introduced.

Acknowledgement

D. A. Humphreys, D. Schreurs and G. Bosi were supported by the European Metrology Research Programme (EMRP) SIB62 Joint Research Project, “HF Circuits”. The EMRP was funded by the EMRP participating countries within EURAMET and the European Union. D. A. Humphreys was also supported by the EMRP IND51 “MORSE” and by the National Measurement Office, an Executive Agency of the U.K. Department for Business, Innovation and Skills. K. N. Gebremicael was supported by the U.K. Engineering and Physical Sciences Research Council Centre for Doctoral Training in Communications under Grants EP/I028153/1, EP/K035746/1 and Roke Manor Research Ltd, UK. KU Leuven also acknowledges FWO and Hercules.

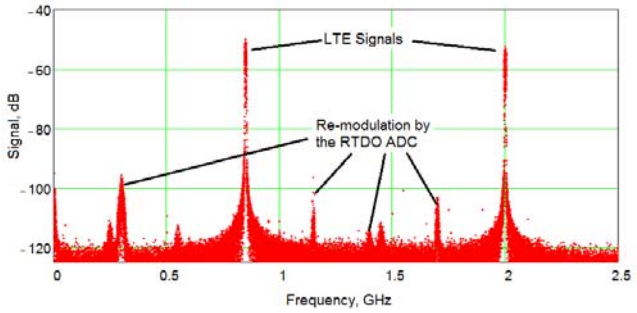

Fig. 6. Frequency components of the LTE waveform showing signal components and DRTO artifacts.

References

[1] M. R. Harper, A. J. A. Smith, A. Basu, and D. A. Humphreys, “Calibration of a 70 GHz Oscilloscope,” CPEM 2004, London, June 27 - July 2, 2004, pp. 530-531.

[2] D. F. Williams, P. D. Hale, T. S. Clement, and J. M. Morgan, “Calibrating electro-optic sampling systems,” IMS Conference Digest, pp. 1527-1530, May 2001.

[3] M. Bieler, M. Spitzer, K. Pierz, and U. Siegner, “Improved Optoelectronic Technique for the time-domain Characterization of sampling oscilloscopes,” IEEE Trans. Instrum. Meas., vol. 58, no. 4, pp. 1065-1071, Apr. 2009.

[4] D A Humphreys, “Vector Measurement of Modulated RF Signals by an In-Phase and Quadrature Referencing Technique,” IET Proc. Sci. Meas. Tech, BEMC Special edition, IEE vol. 153, no. 6, pp. 210-216, Nov. 2006.

[5] P. D. Hale, C. M. Wang, D. F. Williams, K. A. Remley, and J. Wepman, “Compensation of random and systematic timing errors in sampling oscilloscopes,” IEEE Trans. Instrum. Meas., vol. 55, no. 6, pp. 2146-2154, Dec. 2006.

[6] G Vandersteen, Y Rolain, and J Schoukens, “An identification technique for data acquisition characterization in the presence of nonlinear distortions and time base distortions,” IEEE Trans. Instrum. Meas., vol. 50, no. 5, pp.1355 – 1363, Oct. 2001.

[7] D. Humphreys, M. Akmal, “Channel timebase errors for Digital Sampling Oscilloscopes,” Conference on Precision Electromagnetic Measurements (CPEM), pp.520-521, 1-6 July 2012.

[8] W.C. Black and D. Hodges, “Time interleaved converter arrays,” IEEE J. Solid-State Circuits, vol. 15, no. 6, pp. 1022 – 1029, Dec. 1980.

[9] D.A. Humphreys, M. Hudlicka, I. Fatadin, “Calibration of Wideband Digital Real-Time Oscilloscopes,” IEEE Trans. Instrum. Meas., vol. 64, no.6, pp.1716 – 1725, June 2015.

[10] C. Cho, J.-G. Lee, P. D. Hale, J. A. Jargon, P. Jeavons, J. Schlager, and A. Dienstfrey, “Calibration of channel mismatch in time-interleaved real-time digital oscilloscopes,” in 85th ARFTG Microw. Meas. Conf. Dig., May. 2015, pp. 1–5.

[11] S. Gustafsson, M. Thorsell, J. Stenarson, and C. Fager, “An Oscilloscope Correction Method for Vector-Corrected RF Measurements,” IEEE Trans. Instrum. Meas., vol. 64, no. 9, Sept. 2015.

[12] M. Mishali and Y.C. Eldar, “From Theory to Practice: Sub-Nyquist Sampling of Sparse Wideband Analog Signals,” IEEE J. Selected Topics in Sig. Proc., vol.4, no.2, pp.375-391, April 2010.